Journal of Ginseng Research 49 (2025) 53–63

Contents lists available at ScienceDirect

Journal of Ginseng Research

journal homepage: www.sciencedirect.com/journal/journal-of-ginseng-research

Research Article

Non-saponin from *Panax ginseng* maintains blood-brain barrier integrity by inhibiting NF-κB and p38 MAP kinase signaling pathways to prevent the progression of experimental autoimmune encephalomyelitis

Jinhee Oh [a,b,1], Yujeong Ha [a,b,1], Tae Woo Kwon [a,b], Hyo-Sung Jo [a,b], Sang-Kwan Moon [c], Yoonsung Lee [d], Seung-Yeol Nah [e], Min Soo Kim [f,g], Ik-Hyun Cho [a,b,g,*]

[a] Department of Convergence Medical Science, College of Korean Medicine, Kyung Hee University, Seoul, Republic of Korea
[b] Department of Science in Korean Medicine, Graduate School, Kyung Hee University, Seoul, Republic of Korea
[c] Department of Clinical Korean Medicine, Graduate School, Kyung Hee University, Seoul, Republic of Korea
[d] Clinical Research Institute, Kyung Hee University Hospital at Gangdong, School of Medicine, Kyung Hee University, Seoul, Republic of Korea
[e] Ginsentology Research Laboratory and Department of Physiology, College of Veterinary Medicine and Bio/Molecular Informatics Center, Konkuk University, Seoul, Republic of Korea
[f] Brain Science Institute, Korea Institute of Science and Technology (KIST), Seoul, Republic of Korea
[g] KHU-KIST Department of Converging Science and Technology, Kyung Hee University, Seoul, Republic of Korea

ARTICLE INFO

Keywords:
Non-saponin
Multiple sclerosis
Experimental autoimmune encephalomyelitis
Blood-brain barrier
Nuclear factor kappa B
p38 mitogen-activated protein kinase

ABSTRACT

Background: The non-saponin (NS) fraction is an important active component of *Panax ginseng*, with multi-functional pharmacological activities including neuroprotective, immune regulatory, anti-inflammatory, and antioxidant effects. However, the effects of NSs on multiple sclerosis (MS), a chronic and autoimmune demyelinating disorder, have not yet been demonstrated.

Purpose: and Methods: The goal of the present study was to demonstrate the pharmacological actions of NSs on movement dysfunctions and the related mechanisms of action using an experimental autoimmune encephalomyelitis (EAE) mouse model of MS.

Results: NSs (p.o.) alleviated movement dysfunctions in EAE mice related to reduced demyelination in the lumbar spinal cord (LSC). NSs attenuated the recruitment of microglia ($CD11b^{+}/CD45^{low}$) and macrophages ($CD11b^{+}/CD45^{high}$) in LSCs from EAE model mice, consistent with the decreased mRNA expression levels of the main proinflammatory mediators (IL-1β, COX-2, MCP-1, MIP-1α, and RANTES). NSs blocked the migration of Th17 cells ($CD4^{+}/IL17A^{+}$) and mRNA expression levels of IL-17A (product of Th17 cells) in LSCs from EAE mice. NSs suppressed alterations in blood-brain barrier (BBB) components, such as astrocytes and cell adhesion molecules, associated with inhibiting NF-κB and p38 MAPK pathways in LSCs of EAE mice and lipopolysaccharide-induced bEND.3 cells.

Conclusions: NSs could attenuate movement dysfunctions and related pathological/inflammatory changes by reducing BBB permeability through NF-κB and p38 MAPK pathway inhibition in LSCs of EAE model mice. These are the first results suggesting that NSs can be potential therapeutic agents for MS by reducing BBB permeability.

1. Introduction

Multiple sclerosis (MS) is an autoimmune disorder of the central nervous system characterized by chronic inflammation, demyelination, gliosis, and neuronal death. It is the most common neurological disorder that usually occurs between the ages of 20 and 40 years [1–3]. Its typical neurobehavioral signs include tetraplegia, dyschezia, weakness, lazy eye, and ataxia [1–3]. Although the pathogenesis of MS is unclear, its etiology is multifactorial and includes genetic, environmental, and mixed factors [4]. These factors can trigger a cascade of events in the neuroimmune system from the periphery through the blood-brain barrier (BBB), generating neurodegeneration (degeneration of myelin and

* Corresponding author. Department of Convergence Medical Science, College of Korean Medicine, Kyung Hee University, Seoul, 02447, Republic of Korea.
E-mail address: ihcho@khu.ac.kr (I.-H. Cho).
[1] These authors contributed equally to this work.

https://doi.org/10.1016/j.jgr.2024.09.005
Received 4 June 2024; Received in revised form 7 August 2024; Accepted 19 September 2024
Available online 26 September 2024

oligodendrocytes) [1–3]. Since most (>85 %) patients present with the most common two types of MS (relapsing-remitting MS and secondary-progressive MS), the current medicines (e.g., fingolimod, interferon-beta, and glatiramer acetate) target these types [2,5,6]. Recently, both the United States Food and Drug Administration and the European Medicines Agency approved ocrelizumab for treating primary-progressive MS [7]. All of these drugs, including orelizumab, only can delay MS's progression and relieve its symptoms but also have various adverse effects [2]. For example, laquinimod can produce coughing, headache, and nausea. Glatiramer acetate can induce anxiety, rubeosis, and hives. Daclizumab can increase liver enzymes and cutaneous reactions [2,5,6]. Currently, there is no definite cure for the multifactorial cause of MS.

Although nuclear factor kappa B (NF-κB) and p38 mitogen-activated protein kinase (MAPK) pathways can be importantly involved in the etiology of MS and experimental autoimmune encephalomyelitis (EAE), a rodent model of MS [8–12], their roles remain to be elucidated. Upon activation, the NF-κB and p38 MAPK pathways increase inflammatory cytokines interleukin-1 beta (IL-1β) and tumor necrosis factor-alpha (TNF)-α, reactive nitrogen species, and reactive oxygen species (ROS), which injures oligodendrocytes and neurons and, thus, cause demyelination [13]. Both pathways can also enhance BBB permeability or damage the BBB by increasing the expression of cell adhesion molecules [platelet endothelial cell adhesion molecule-1 (PECAM-1 or CD31), intercellular adhesion molecule-1 (ICAM-1), and vascular cell adhesion molecules-1 (VCAM-1)] and decreasing tight junctional molecules [occludins and claudins] upon induction by pathogen-associated molecular patterns (PAMPs) and endogenous danger-associated molecular patterns (DAMPs) [14,15]. Enhanced BBB permeability can trigger or aggravate MS and EAE [14,15]. According to accumulated reports, inhibitors and genetic mutations in NF-κB and p38 MAPK pathways might prevent, slow, or inhibit the onset or deterioration of MS or EAE related to BBB malfunction [8–12]. Thus, agents regulating NF-κB and p38 MAPK pathways may be attractive treatments for MS by decreasing BBB permeability. Recently, plant-derived natural products (foods and medicines) have become increasingly popular due to their safety, physical strength enhancement, and excellent effectiveness in treating diseases [16,17]. *Panax ginseng (P. ginseng)*, also known as Korean ginseng, is a traditional Oriental herbal medicine that has been used for thousands of years as a blood-nourishing tonic in countries such as Korea, China, and Japan [18–20]. It has exhibited various biological and pharmacological effects, including antioxidant, anti-inflammatory, vasorelaxation, immune-boosting, and anticancer/neuroprotective activities *in vitro, in vivo,* and in clinical studies [18–20]. The distinct bioactive activity of *P. ginseng* is not due to one or two specific components but to the complex action of a wide range of saponin and non-saponin (NS) components. Therefore, investigating the action of saponin or NSs is more important than that of individual components [21]. The NS components of *P. ginseng* are classified into polysaccharides, nitrogen compounds (amino acids, peptides, proteins, alkaloids, and nucleic acids), and fat-soluble components (polyacetylene, phenols, essential oils, and phytosterols) [21]. An NS containing polysaccharides and panaxcerol D (a kind of glycosyl glyceride) showed therapeutic action in a murine model of Alzheimer's disease (AD) by regulating synaptic- and mitochondrial-related pathways [22], targeting tau pathology [23] and improving cholinergic blockade or Aβ accumulation [24]. An NS promoted the proliferation of primary oligodendrocyte precursor cells and prevented their death under oxidative stress [25]. Arginyl-fructosyl-glucose alleviated D-galactose-induced aging in mice by correcting mitochondrial dysfunction caused by ROS accumulation [26]. Arginyl-fructosyl-glucose and maltol derivatives exhibited high antioxidant, anti-apoptotic, and neuroprotective actions [27–29]. These studies suggest that NSs have the potential for use in multi-targeted approaches to treat MS. However, their molecular mechanism is less clear compared to other saponin fractions or individual ginsenosides. The roles of NSs in the context of MS, an autoimmune-related disorder of the nervous system, are also presently unknown. To the best of our knowledge, this was the first study to confirm a positive effect of NSs in alleviating movement dysfunction by attenuating demyelination, inflammation, and BBB breakdown by down-regulating the NF-κB p65 and p38 MAPK pathways in an EAE murine model.

2. Materials and methods

2.1. Reagents

NS fraction was provided from Korean Society of Ginseng (Seoul, Republic of Korea). NS fraction was prepared from red ginseng extract [30,31]. NS fraction contained polysaccharides [galacturonic acid (25.23 mg/g) + galactose (18.90 mg/g) + arabinose (13.80 mg/g) = 56.20 mg/g], arginyl-fructosyl-glucose (17.94 mg/g), and free sugars [glucose (1.22 %) + fructose (1.83 %) + sucrose (5.63 %) + maltose (6.05 %) = 14.73 %]. Main ginsenosides (Rg_1, Re, Rf, Rh_1, Rg_{2s}, Rb_1, Rc, Rb_2, Rd, Rg_{3s}, and Rg_{3r}) were not detected in NS fraction. Eosin (45, 260), Freund's adjuvant (F5881, CFA), hematoxylin (H3138), lipopolysaccharide (L3129, 0127:B8, LPS), luxol fast blue (L0294, LFB), myelin oligodendrocyte glycoprotein (163,913-87-9, MOG_{35-55} peptide, paraformaldehyde (158,127, PFA), pertussis toxin (P7208, PTX), and tween 80 (P1754) were purchased from Sigma-Aldrich (St. Louis, MO). bEND.3 cell line (CRL-2299) was purchased from the ATCC (Manassas, VA). *Mycobacterium tuberculosis* H37Ra (BD 231141) was purchased from BD Difco (Detroit, MI). Primary antibodies: Rabbit anti-ionized calcium binding adaptor molecule-1 (019–19741, Iba-1) was purchased from Wako Pure Chemical Industries Ltd. (Osaka, Japan). Rabbit anti-glial fibrillary acidic protein (GA52461-2, GFAP) was purchased from Dako Products (Carpinteria, CA). Rat anti-myelin binding protein (ab7349, MBP) was purchased from Abcam (Cambridge, UK). Rat anti-platelet endothelial cell adhesion molecule-1 (sc-46694, PECAM-1) was purchased from Santa Cruz Biotechnology (Santa Cruz, CA). Rabbit anti-phospho (p)-NF-κB p65 (sc-101752), rabbit anti-NF-κB p65 (sc-7151), rabbit anti-p-p38 (sc-101758), and rabbit anti-p38 (9212) were purchased from Cell Signaling Technology (Beverly, MA). Secondary antibodies; cyanine 3 (128-165-160, Cy3)- and fluorescein-isothiocyanate (128-095-160, FITC)-conjugated rabbit/rat/mouse IgG were purchased from Jackson ImmunoResearch Inc. (West Grove, PA). Biotinylated rabbit/rat/mouse IgG (BA-1000; BA-9400; BA-2000) and horseradish peroxidase (HRP)-conjugated secondary antibodies (A-2014) and avidin-biotinylated HRP-complex (A-2004, ABC) were purchased from Vector Laboratories (Burlingame, PA).

2.2. Animals and ethics statement

Nine weeks old female C57BL/6 mice (weight, 19–21 g; Narabiotechnology Co., Ltd., Pyeongtaek, Republic of Korea) were kept at a 12h light-dark cycle (light on 07:00 to 19:00) at room temperature (23 ± 3 °C) and humidity (55 ± 5 %). Their seed mice were originated from Taconic Biosciences Inc. (Cambridge, IN). Mice from different experimental groups were mixed in the cages. The mice were allowed to consume food and water *ad libitum* and were habituated to the housing facilities for 1 week before the experiments. All experimental procedures were reviewed and approved by the Institutional Animal Care and Use Committee (IACUC) of Kyung Hee University (KHUASP(SE)-18-174; Approval date, Jan 23, 2019). In this process, proper randomization of laboratory animals and handling of data were performed in a blinded manner in accordance with recent recommendations from a National Institutes of Health Workshop on preclinical models of neurological diseases [32].

2.3. Experimental groups and NS treatment

To demonstrate whether NS has a positive efficacy of NS on EAE,

mice were randomly divided into the following 6 groups (n = 8 per group): 1) Sham [vehicle treatment (s.c.) + saline (p.o.)]; 2) EAE [MOG_{35-55} immunization (s.c.) + saline (p.o.)]; 3) EAE + NS [MOG_{35-55} immunization (s.c.) + NS (100, 200, and 400 mg/kg) (p.o.)]; and 4) NS [vehicle treatment (s.c.) + NS 400 mg/kg (p.o.)]. The mice were orally (p.o.) pretreated with NS daily from 4 days before immunization to the end of experiment (Fig. 1A).

2.4. EAE model induction and evaluation of movement dysfunction

EAE model were induced as previously described [20,33,34]. Briefly, mice were immunized subcutaneously (s.c.) with 100 μl of an emulsion containing 200 μg of MOG_{35-55} peptide in phosphate buffered saline (PBS), equivalent volumes of CFA, and 550 μg of *Mycobacterium tuberculosis* H37Ra into the hind flanks. Mice received 250 ng of PTX in 100 μl PBS by intraperitoneal (i.p.) injection on day 0 and 2 after immunization (Fig. 1A). The movement dysfunction grade was evaluated daily in all groups after immunization as previously described [33–36].

2.5. Histopathological examination

Seventeen days after EAE induction, mice (n = 5 per group) were deeply anesthetized with 2 % isoflurane, and perfused intracardially with 0.9 % physiological saline followed by 4 % PFA in 0.1M phosphate buffer (pH 7.4). Lumbar spinal cords (LSCs; L4-5) were removed and post-fixed in perfusate for more overnight, then cryo-sections (10-μm thick; n = 3 per LSC) were prepared by previous described [36,37]. The sections were stained with LFB and hematoxylin and eosin (H&E) to investigate level of demyelination and inflammatory cell infiltration, respectively, by previously described [36,37]. The level of demyelination and infiltration of immune cells was scored as described previously [37,38].

2.6. Immunohistochemistry and immunofluorescence evaluation

Immunohistochemical staining was performed using the cryo-sections prepared above as previously described [36,37]. Briefly, sections (10-μm thickness; sections per LSC; 5 LSCs per group) from LSCs in all groups were incubated with rabbit anti-Iba-1 (1:1,000) and rabbit anti-GFAP (1:3,000) as primary antibodies and biotinylated rabbit IgG (1:500) as secondary antibody. The sections were incubated avidin-biotinylated HRP-complex and visualized with 3, 3′-diamino-benzidine. Immunofluorescence staining was conducted as previously described [36,37]. Briefly, sections (10-μm thick; 3 sections per LSC; 5 LSCs per group) from LSCs in all groups were incubated with rat anti-MBP (1:1,000) and rat anti-PECAM-1 (1:1000) as primary antibodies and then Cy3-and FITC-conjugated rat IgG (1:1500) as secondary antibodies. Stained sections were examined and digitized with Zeiss LSM Pascal 5 Confocal Laser Scanning Microscope (Carl Zeiss, Oberkochen, Germany).

2.7. Western blot analysis

Seventeen days after EAE induction, the LSCs (n = 5 per group) from all groups were rapidly cropped under 2 % isoflurane anesthesia. Western blot was conducted by previous described [35–37]. The following primary antibodies were used: rat anti-MBP (1:1,000), rabbit anti-Iba-1 (1:1,000), mouse anti-GFAP (1:5,000), rat anti-PECAM-1 (1:1,000), rabbit anti-p-NF-κB p65 (1:700), rabbit anti-p-p38 (1:700) or HRP-conjugated secondary antibodies (1:500). For normalization of the antibody signal, the membranes were stripped and reprobed with β-actin (1:500), glyceraldehyde 3-phosphate dehydrogenase (GAPDH; 1:2000) or total antibody against each protein (1:1000). Western blot was conducted at least three trials. PVDF membranes were visualized and quantified by previous described [37,39].

2.8. Reverse transcription-polymerase chain reaction (RT-PCR) and real-time PCR

Seventeen days after EAE induction, the LSCs (n = 5 per group) from all groups were rapidly cropped under 2 % isoflurane anesthesia. RT-PCR and real time PCR assays were performed by previous described [35–37]. All PCR experiments were repeated at least three times. Real-time PCR analysis was accomplished using SYBR Green PCR Master Mix (Applied Biosystems, Franklin Lakes, NJ). The primer sequences were as follows: Cyclooxygenase (COX)-2-5′-CAG TAT CAG AAC CGC ATT GCC-3′ and 5′-GAG CAA GTC CGT GTT CAA GGA-3′, Intercellular adhesion molecule (ICAM)-1-5′-TGC GTT TTG GAG CTA GCG GAC CA-3′ and 5′-CGA GGA CCA TAC AGC ACG TGC AG-3′, Interferon gamma (IFN)-γ-5′-ACA ATG AAC GCT ACA CAC TGC AT-3′ and 5′-TGG CAG TAA CAG CCA GAA ACA-3′, IL-17A-5′-GTG TCT CTG ATG CTG TTG-3′ and 5′-AAC GGT TGA GGT AGT CTG-3′, IL-1β-5′-TTG TGG CTG TGG AGA AGC TGT-3′ and 5′-AAC GTC ACA CAC CAG CAG GTT-3′, Monocyte chemoattractant protein (MCP)-1-5′-CTT CTG GGC CTG CTG TTC A-3′ and 5′-CCA GCC TAC TCA TTG GGA TCA-3′, Macrophage inflammatory protein (MIP)-1α-5′-CAG CCA GGT GTC ATT TTC CT-3′ and 5′-AGG CAT TCA GTT CCA GGT CA-3′, Occludin-5′-ATG CAT CTC TCC GCC ATA CAT-3′ and 5′-AGA CCT GAT GAA TTC AAA CCC AAT-3′, Regulated on activation, normal T-cell expressed and secreted (RANTES)-5′-ACA CCA CTC CCT GCT GCT TT-3′ and 5′-GAC TGC AAG ATT GGA GCA CTT GA-3′, and Vascular cell adhesion molecule (VCAM)-1-5′-CCT CAC TTG CAG CAC TAC GGG CT-3′ and 5′-TTT TCC AAT ATC CTC AAT GAC GGG-3′.

2.9. Flow cytometry

Seventeen days after EAE induction, mice (n = 5 per group) with average movement dysfunction in each group were rapidly perfused intracardially with saline and LSCs were carefully cropped under 2 % isoflurane anesthesia. To examine the level of recruitment of resident microglia ($CD11b^+/CD45^{low}$), peripheral macrophage ($CD11b^+/CD45^{high}$), Th1 ($CD4^+/IFN\text{-}\gamma^+$), and Th17 ($CD4^+/IL17A^+$) cells, flow cytometry was performed using a previously described method [35,36,39]. Briefly, after acquiring unstained and single colored control samples to calculate the compensation matrix, $1x10^4$ events were acquired within the combined gate based on physical parameters [forward scatter (FSC) and side scatter (SSC)].

2.10. bEND.3 cell culture

bEND.3 cell line, endothelial cells isolated from brain tissue derived from a mouse with endothelioma, was cultured as previous described [33]. Cultured cells were pretreated with NS (50, 100, and 200 μg/mL) for 1 h followed by treatment with LPS for 4 h to examine the effect of NSs on BBB integrity. Cells were then collected for Western blot analysis.

2.11. Statistical analysis

Statistical analysis was performed using SPSS statistical package version 25.0 (IBM SPSS Inc., New York, NY). Movement dysfunction scores obtained after EAE induction were analyzed using two-way analysis of variance (ANOVA) with repeated measures using one within-subjects factor (day) and two between-subject factors (sham and EAE groups; EAE and EAE + NS groups). All other experimental data were analyzed using one-way ANOVA with Tukey *post hoc* test for comparison of multiple groups. All of the data were presented as mean ± standard error of the mean (SEM). The p-values of less than 0.05 were accepted as statistically significant.

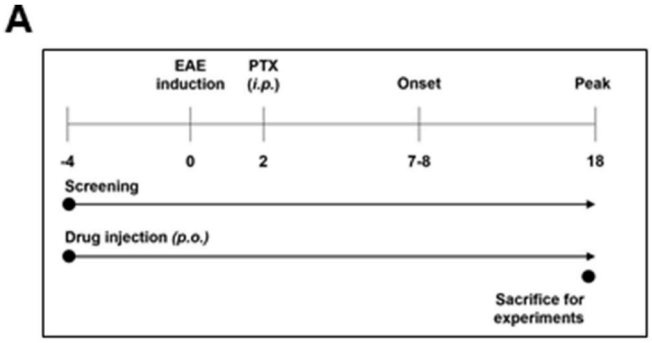

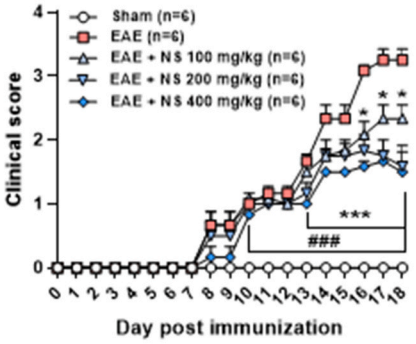

C

Groups	Incidence	EAE onset (d.p.i)	Maximum behavioral score
EAE	6/6	7.7±0.4	3.3±0.2
EAE + NS 100	6/6	7.7±0.4	2.3±0.2***
EAE + NS 200	6/6	8.0±0.4	1.9±0.2***
EAE + NS 400	6/6	8.8±0.4	1.7±0.2***

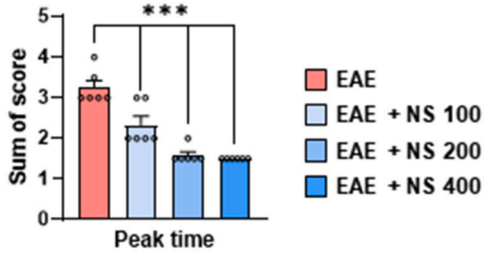

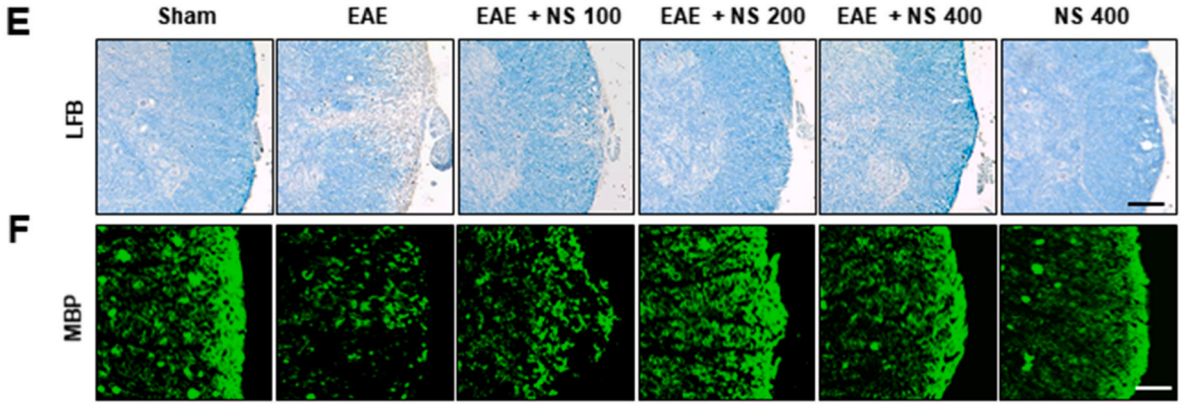

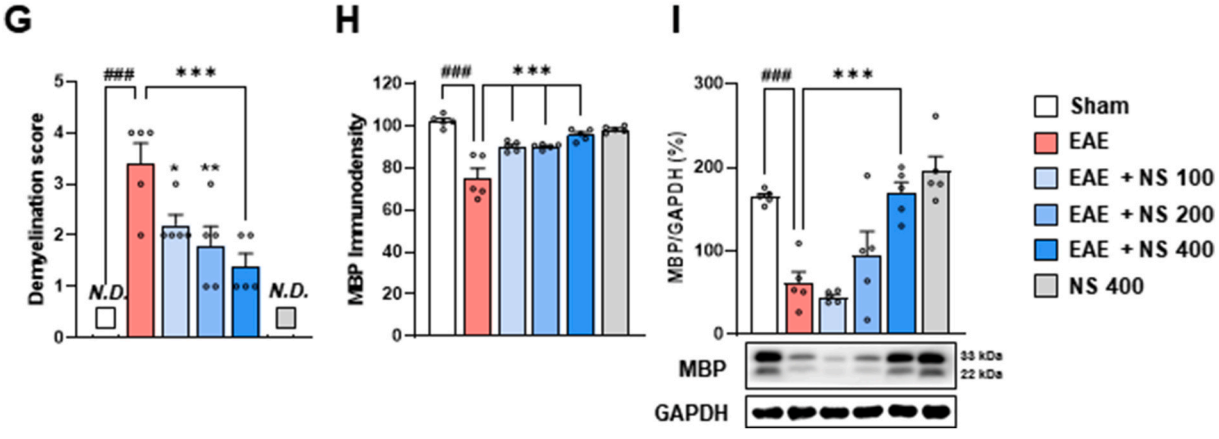

(caption on next page)

Fig. 1. NS blocked the progression of motor impairment and demyelination in LSCs from the EAE group.
(A) The experimental design and schedule. The EAE and EAE + NS groups were induced (s.c.) with an emulsion containing MOG_{35-55} peptide, CFA, and *Mycobacterium tuberculosis*. The Sham and NS alone groups were administered equivalent volumes of the vehicle. Behavioral tests were conducted daily and sampling was performed immediately after the last behavioral test. **(B)** After EAE induction, motor impairment was recorded in the Sham, EAE (n = 6), EAE + NS (100, 200, or 400 mg/kg; n = 8 per group), and NS (400 mg/kg; n = 8) groups daily for 17 days. **(C)** The incidence of EAE (spiritless tail), date of appearance of neurological signs (onset), and maximum behavioral score (calculated by adding maximum scores of individual diseased mice and divided by the number of diseased mice) are displayed as means ± S.E.M. **(D)** Sum of clinical scores from day 8–17 post-immunization. **(F–I)** Cryo-sections (n = 3 per LSC) of LSCs from all groups (n = 5 per group) were subjected to LFB staining (F) and immunofluorescence staining using *anti*-MBP antibody (G). G and H are quantified graphs of E and F, respectively. **(I)** LSC lysates from all groups (n = 5 per group) were subjected to Western blot analysis for MBP protein analysis and then quantified to assess the severity of neurodegeneration (demyelination). Bars = 100 μm. Data are expressed as mean behavioral scores or mean expressive value ± SEM (two-way ANOVA for A; one-way ANOVA for E and F; #$p < 0.05$, ##$p < 0.01$, and ###$p < 0.001$ vs. sham group; *$p < 0.05$, **$p < 0.01$, and ***$p < 0.001$ vs. EAE group). ANOVA, Analysis of variance; CFA, Complete Freund's adjuvant; EAE, Experimental autoimmune encephalomyelitis; LFB, Luxol fast blue; LSCs, Lumbar spinal cords; MBP, Myelin binding protein; MOG, Myelin oligodendrocyte glycoprotein; N.D., Not detected; NS, Non-saponin; SEM, Standard error of the mean.

3. Results

3.1. NS alleviates movement dysfunctions and demyelination in LSCs from the EAE group

Generally, movement dysfunctions in MS and the EAE model are closely related to myelin degeneration in the spinal cord [1–3]. First, we investigated the effects of NS on movement dysfunctions and demyelination in LSCs from the EAE group (Fig. 1A and B). Early movement dysfunctions (partial loss of tail tone and tail paralysis) were observed 7.7 ± 0.4 days after in EAE group, whereas the onset was delayed by 8.8 ± 0.4 days in groups administered 400 mg/kg of NS (Fig. 1B and C). The movement dysfunctions gradually worsened by 17 days (Fig. 1B). In the EAE group, the mean maxim score was 3.3 ± 0.2 on day 17 after EAE induction. However, when NS was administered daily at 100, 200, and 400 mg/kg, the mean maximum scores were 2.3 ± 0.2, 1.9 ± 0.2, and 1.7 ± 0.2, respectively (Fig. 2B and C). The average accumulative score between day 8 and day 17 was 19.5 ± 0.7 in the EAE group, whereas the scores were 14.0 ± 0.9, 9.5 ± 0.9, and 9.0 ± 0.9 in groups administered 100, 200, and 400 mg/kg of NS, respectively (Fig. 2D). We investigated histopathological changes by LFB staining (Fig. 2E and G) to investigate if the worsening and mitigating of movement dysfunctions were related to the grade of demyelination in the LSCs. Severe demyelination was observed in the EAE group (demyelination score: 3.25 ± 0.4), which was clearly prevented in the NS (400 mg/kg)-administered group (demyelination score: 1.5 ± 0.3) (Fig. 2E and G). Cryo-sections and LSC lysates were subjected to immunofluorescence staining and Western blot assays for MBP, respectively, to further investigate the severity of demyelination. MBP is the second most abundant protein in myelin in the nervous system (Fig. 1F and H). Changes in MBP-immunoreactivity and its protein expression levels were consistent with LFB staining results (Fig. 1E–I).

3.2. NS decreases the infiltration of inflammatory cells in LSCs from the EAE group

Since histopathological changes (myelin degeneration) in the EAE model are featured by recruitment and the infiltration of inflammatory cells [1–3], we conducted H&E staining to evaluate the changes (Fig. 2A and C). The grade of cell recruitment and infiltration increased in LSCs in the EAE group (inflammation score: 3.3 ± 1.5) depending on the severity of demyelination (Fig. 1E–I), whereas increases were remarkedly prevented in the 200 and 400 mg/kg NS-treated groups (inflammation score: 2.0 ± 0.2 and 1.5 ± 0.2, respectively) (Fig. 2A and C). Myeloid cells (microglia and macrophages) are immune cells that can travel around and inside the neurodegenerating or neoroinflammatory sites in the brain or spinal cord. Both infiltrated cell types are activated and pivotally involved in myelin degeneration in MS and EAE [1–3]. Therefore, we evaluated the levels of infiltration and activation of both cell types (Fig. 2B–G). Iba-1 immunoreactivity intensity was strongly increased in LSCs from the EAE group (20.4 ± 3.7). However, such increases were clearly prevented by NS administration (7.4 ± 1.5 and 5.8 ± 1.0 in 200 and 400 mg/kg, respectively) in a dose-dependent manner (Fig. 2B and D). Consistent with this pattern, Western blot analysis showed that the expression level of Iba-1 protein was clearly enhanced in LSCs from the EAE group (116.8 ± 7.7) compared to the Sham group (2.8 ± 0.5). These increases were significantly prevented by NS administration (80.5 ± 9.6 and 27.1 ± 0.3 in 200 and 400 mg/kg, respectively) in a dose-dependent manner (Fig. 2E). Since the Iba-1 antiserum detects both microglia and macrophages, which have the same origin and similar phenotypes [40], flow cytometry was performed to differentiate the cell types (Fig. 2F and G). The proportion of $CD11b^{+}/CD45^{+(low)}$ cells (R3 region in Fig. 2F) representing microglia was enhanced to 15.1 ± 1.4 % in LSCs from the EAE group, whereas it was significantly lowered to 5.9 ± 1.0 % in LSCs from the EAE group administered 400 mg/kg of NS (Fig. 2F and G). The proportion of $CD11b^{+}/CD45^{+(high)}$ cells (R4 region in Fig. 2F), representing macrophages, was enhanced to 9.8 ± 1.3 % in LSCs from the EAE group. However, the proportion was significantly lowered to 2.0 ± 1.1 % in the EAE group administered 400 mg/kg of NS (Fig. 2F and G).

3.3. NS decreases the expression of proinflammatory mediators in LSCs from the EAE group

The continuous dysregulation of proinflammatory mediators (cytokines and chemokines) and MS conditions may result in neurotoxicity, neuroinflammation and neurodegeneration in the nervous system [1–3]. Hence, we evaluated the mRNA expression grades of representative proinflammatory mediators using the RT-PCR assay (Fig. 3). The mRNA expression levels of the representative proinflammatory cytokine IL-1β and enzyme COX-2 in LSCs from the EAE group were greatly enhanced to 90.5 ± 5.6 % and 99.6 ± 4.0 %, respectively, compared to the Sham group (7.5 ± 1.5 % and 35.1 ± 2.8 %, respectively). However, their levels were significantly down-regulated to 17.4 ± 1.0 % and 9.7 ± 5.1 %, respectively, in the EAE group administered 400 mg/kg of NS compared to the EAE group (Fig. 2H–J).

The mRNA expression grades of representative proinflammatory chemokines MCP-1, MIP-1α, and RANTES in LSCs from the EAE group were significantly upregulated by 78.2 % ± 8.1 %, 60.2 ± 1.4 %, and 93.2 ± 4.0 %, respectively, compared to those in the Sham group (4.2 ± 2.0 %, 10.1 ± 1.6 %, and 20.5 ± 5.4 %, respectively). However, their grades were significantly downregulated to 12.4 ± 2.8 %, 4.3 ± 2.5 %, and 26.4 ± 0.2 %, respectively, in the group administered 400 mg/kg of NS compared to the EAE group (Fig. 2H and 2K-2M).

3.4. NS decreases the activities of CD4, Th1, and Th17 cells in LSCs from the EAE group

$CD4^{+}$ helper T (Th or T) cells can play a decisive role in the pathogenesis of MS and EAE [41–43]. Thus, flow cytometry was performed on LSCs from all groups to demonstrate the action of NS on the migration of $CD4^{+}$ T cells and effector (Th1 and Th17) subsets into demyelinating lesions (Fig. 3). The proportion of $CD4^{+}$ T cells was clearly enhanced in LSCs from the EAE group (6.6 ± 1.3 %) compared to the Sham group

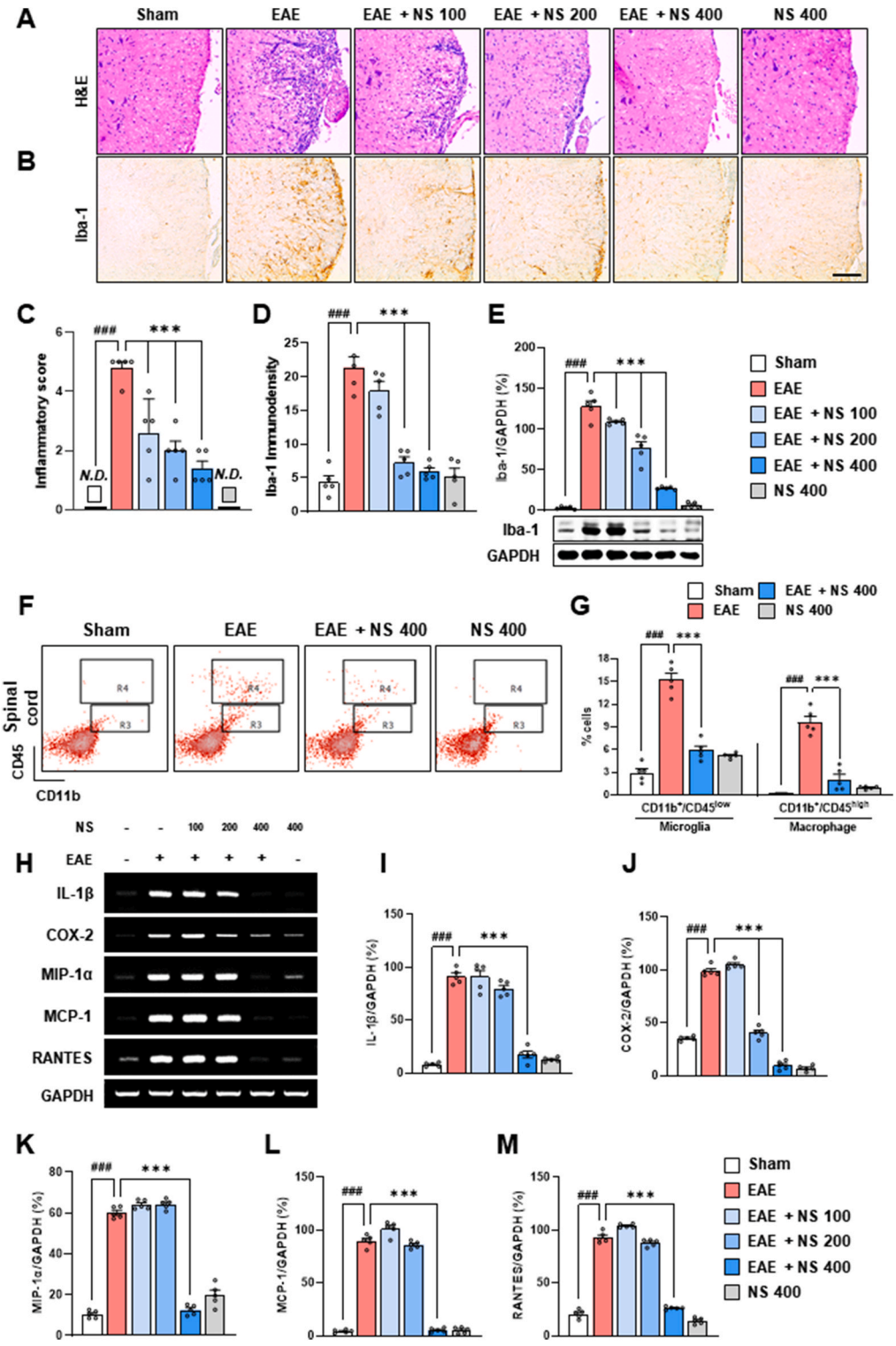

Fig. 2. NS prevented microglia/macrophages infiltration and inflammatory response in LSCs from the EAE group.
Seventeen days following immunization, LSCs were obtained from the Sham, EAE, EAE + NS (100, 200, and 400 mg/kg), and NS (400 mg/kg) alone groups (n = 5 per group). **(A–D)** Cryo-sections (n = 3 per LSC) of LSCs from all groups were subjected to H&E staining (A) and immunohistochemistry (for *anti*-Iba-1 antibody) to measure the infiltration of inflammatory cells (B). C and D are graphs quantifying A and B, respectively. **(E)** LSC lysates (n = 5 per group) were subjected to Western blot analysis to determine and then quantify Iba-1 protein expression levels. **(F and G)** LSCs (n = 5 per group) were subjected to flow cytometry to differentiate infiltrated inflammatory cells. $CD11b^+$ cells were divided into $CD11b^+/CD45^{+(low)}$ cells (R3, microglia) and $CD11b^+/CD45^{+(high)}$ cells (R4, macrophage) proportions (F). Proportion graph of each cell proportion (G). A total of 1 x 10^4 events was acquired from the combined FSC and SSC gates. **(H–M)** LSC lysates (n = 5 per group) were subjected to RT-PCR analysis to quantify the mRNA expression levels of pro-inflammatory cytokine (IL-1β), chemokines (MIP-1α, MCP-1, and RANTES), and an enzyme (COX-2) (H). The results were then quantified (I–M). Bars = 100 μm. Data are expressed as mean expressive value (or the ratio of each value against GAPDH for each sample for C-E and M − N) ± SEM (one-way ANOVA; $\#p < 0.05$, $\#\#p < 0.01$, and $\#\#\#p < 0.001$ vs. sham group; $*p < 0.05$, $**p < 0.01$, and $***p < 0.001$ vs. EAE group). ANOVA, Analysis of variance; EAE, Experimental autoimmune encephalomyelitis; FSC, Forward scatter; LSCs, Lumbar spinal cords; NS, Non-saponin; SEM, Standard error of the mean; SSC, Side scatter.

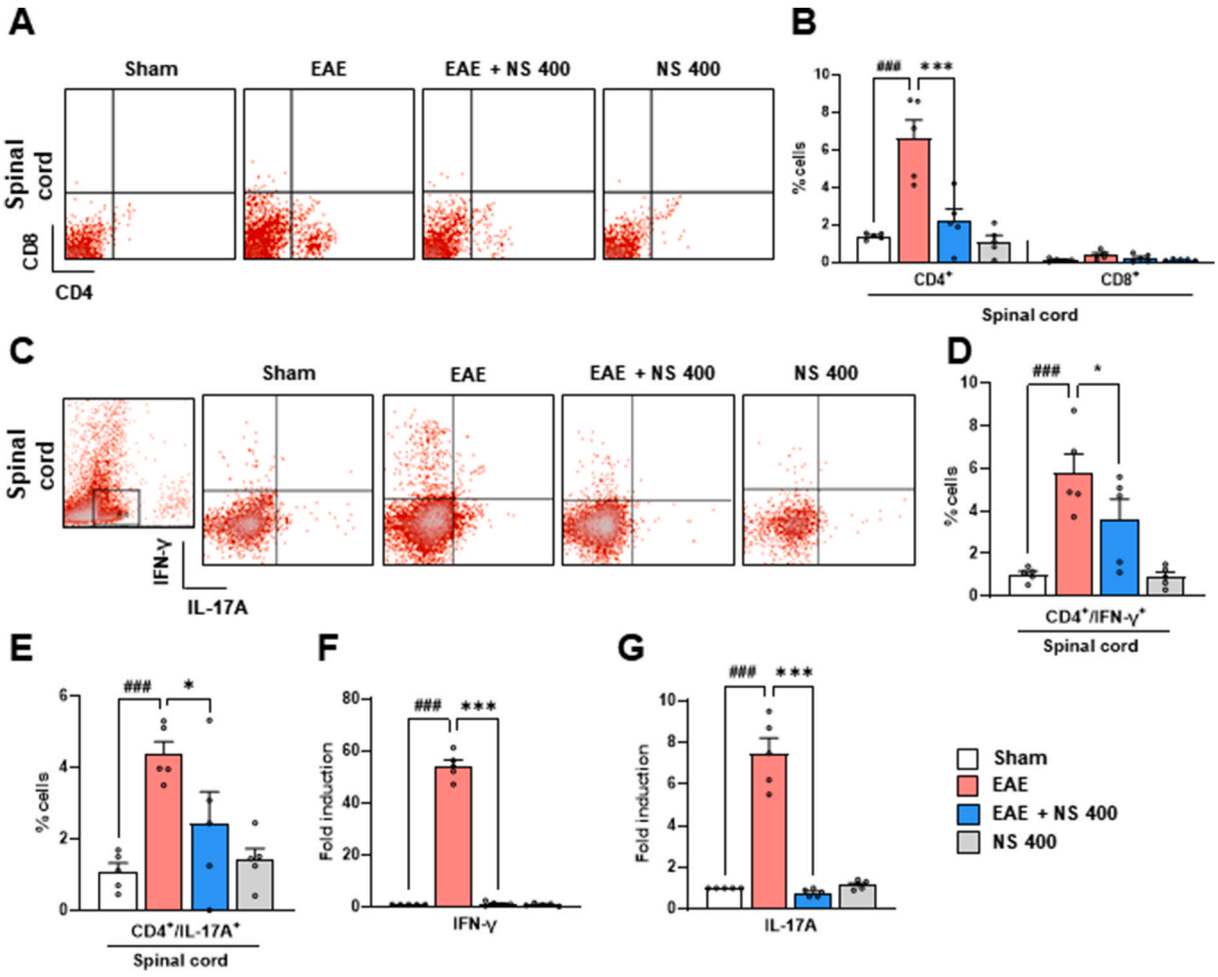

Fig. 3. NS inhibited migration of $CD4^+$ T, Th1, and Th17 cells in LSCs of EAE group.
(A–E) To assess the proportion of Th1 ($CD4^+$/IFN-γ^+) and Th17 ($CD4^+$/IL-$17A^+$) cells by flow cytometry, $CD4^+$ T cells (1×10^4) were first gated using the FSC and SSC properties from the LSCs from each group. The proportions of Th1 and Th17 cells were dotted (C) and plotted in graphs (D and E). **(F and G)** Lysates of LSCs (n = 5) from each group were subjected to real-time PCR assay to evaluate the mRNA expression levels of IFN-γ (F) and IL-17A (G). Quantified data were expressed as mean % cells or fold induction ± SEM. (one-way ANOVA; #$p < 0.05$, ##$p < 0.01$, and ###$p < 0.001$ vs. sham group; *$p < 0.05$, **$p < 0.01$, and ***$p < 0.001$ vs. EAE group). ANOVA, Analysis of variance; EAE, Experimental autoimmune encephalomyelitis; IFN-γ, Interferon gamma; IL, Interleukin; LSCs, Lumbar spinal cords; NS, Non-saponin; PCR, Polymerase chain reaction; SEM, Standard error of the mean.

(1.4 ± 0.1 %), whereas this increase was prevented in LSCs from the 400 mg/kg NS-treated EAE group (2.2 ± 0.2 %) (Figs. 3A and B). The proportion of cytotoxic $CD8^+$ T cells was not prominently regulated by EAE induction or NS administration (Figs. 3A and B). IFN-γ releasing Th1 ($CD4^+$/IFN-γ^+) cells and IL-17 releasing Th17 ($CD4^+$/IL-17^+) cells can play central roles in MS and EAE [41–43]. Thus, the effect of NS on the migration of both effector subsets (Th1 and Th17) was examined in LSCs from all groups. Proportion of Th1 and Th17 cells were enhanced in LSCs from the EAE group (5.8 ± 1.5 % and 4.3 ± 0.4 %, respectively) compared to the Sham group (1.0 ± 0.1 % and 1.1 ± 0.6 %, respectively), while enhancements were significantly prevented in the 400 mg/kg NS-treated EAE group (3.6 ± 1.3 % and 2.3 ± 0.5 %, respectively) compared to the EAE group (Fig. 3C–E). These results were consistent with alterations in the mRNA expression of IFN-γ (an inducer for Th1 cells; an interleukin secreted by Th1 cells) and IL-17 (an interleukin secreted by Th17 cells) (Figs. 3F and G). As expected, proportions of Th1 and Th17 cells and their cytokines (IFN-γ and IL-17) were not significantly altered in the Sham group or the group treated with 400 mg/kg NS alone without EAE induction (Fig. 3C-3G>).

3.5. NSs downregulate the expression of astrocytes and PECAM-1 in LSCs from the EAE group

MS and EAE are characterized by BBB dysfunction and the accumulation of inflammatory infiltrates in the brain and spinal cord [14, 15]. The BBB is composed of endothelial cells, pericytes, and astrocytes, which produce a neurovascular unit with adjacent neurons [14,15]. Therefore, we evaluated changes in these components in LSCs from all groups (Fig.4A–F). The expression of GFAP-immuno-positive astrocytes was notably enhanced in the white matter of LSCs from the EAE group (53.4 ± 3.7) compared to the Sham group (4.2 ± 0.2), whereas its expression was significantly suppressed by 400 mg/kg NS (34.9 ± 0.1) treatment compared with the EAE group (Fig. 4A and C). As expected, these alterations in GFAP protein expression corresponded to the Western blot results (Fig. 4E). PECAM-1 (CD31), an indicator of BBB breakdown, is expressed on endothelial cells and regulates BBB integrity and immune cell trafficking in MS pathogenesis [43]. Therefore, we investigated the effect of NS on PECAM-1 expression in LSCs after EAE induction (Fig. 4B, D, and 4F). The relative intensity of the PECAM-1 immunofluorescence signal was significantly enhanced in LSCs from

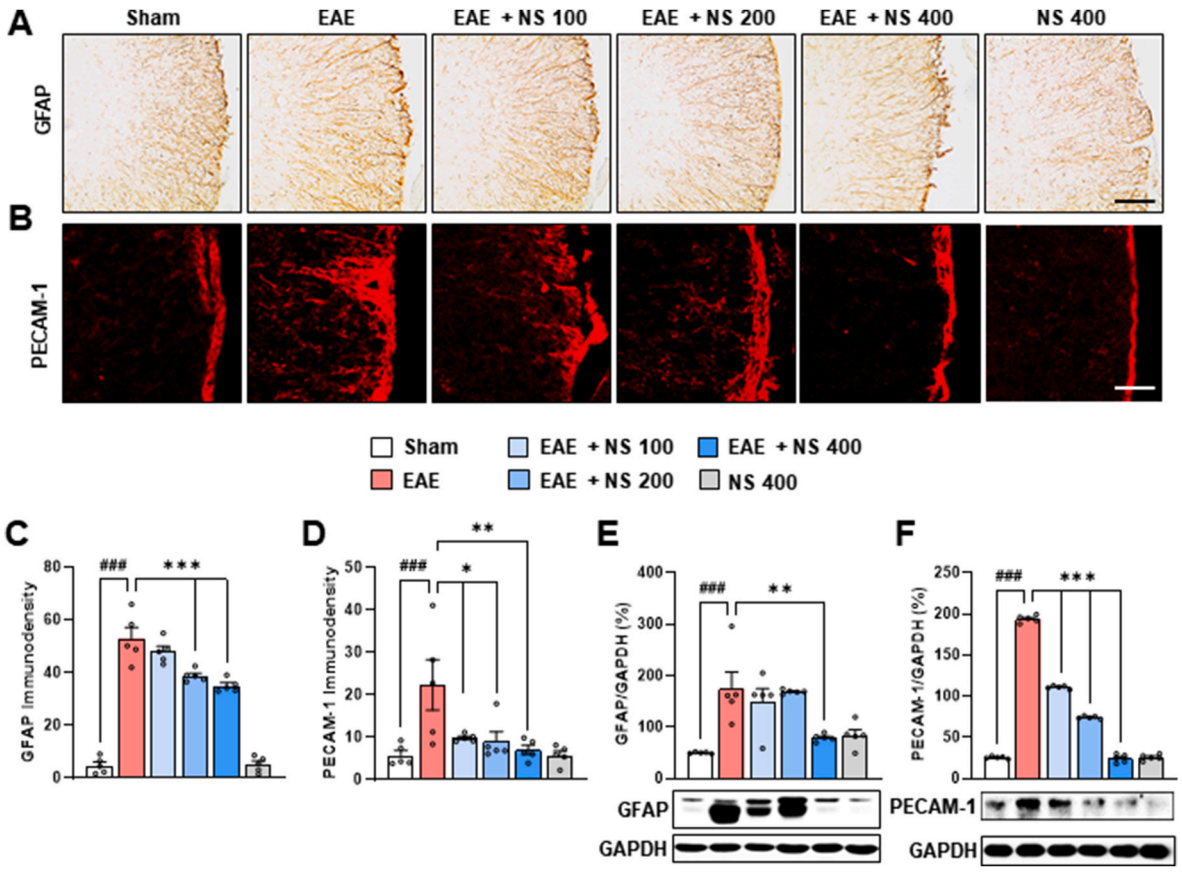

Fig. 4. NS reduced the loss of BBB integrity in LSCs from the EAE group.
At day 17 after immunization, LSCs (n = 5 per group) were harvested from the Sham, EAE, EAE + NS (100, 200, and 400 mg/kg), and NS (400 mg/kg) alone groups. **(A–D)** Cryo-sections (n = 3 per LSC) were subjected to immunohistochemistry with *anti*-GFAP (a marker for astrocytes) (A) and immunofluorescence staining with *anti*-PECAM-1 (a marker for BBB integrity) (B) to investigate alterations in BBB integrity. Their relative intensities were evaluated using the ImageJ program (C and D). **(E and F)** LSC lysates from all groups were examined and quantified for protein expression levels of GFAP (E) and PECAM-1 (F) by Western bolt analysis. Experiments on Western blot were repeated three times. Bar = 100 μm. Data are presented as mean expression values (ratio of each value to GAPDH in each sample). One-way ANOVA; ##$p < 0.01$ vs. sham group; *$p < 0.05$ vs. EAE group). ANOVA, Analysis of variance; BBB, Blood-brain barrier; EAE, Experimental autoimmune encephalomyelitis; GFAP, Glial fibrillary acidic protein; GAPDH, Glyceraldehyde 3-phosphate dehydrogenase; LSCs, Lumbar spinal cords; NS, Non-saponin; PECAM-1, Platelet endothelial cell adhesion molecule-1; SEM, Standard error of the mean.

the EAE group (20.1 ± 4.0) compared to the Sham group (6.3 ± 0.7), whereas the relative intensity was significantly less in groups administered NS in a dose-dependent manner (10.2 ± 1.5, 8.1 ± 0.7 and 7.2 ± 0.4 in 100, 200, and 400 mg/kg NS groups, respectively) compared to the EAE group (Fig. 4B and D). As expected, these alterations in PECAM-1 protein expression corresponded to the Western blot results (Fig. 4F).

3.6. NS inhibits enhancements in adhesion molecules in LPS-stimulated bEND.3 cells

Representative cell adhesion molecules (CAMs), such as ICAM-1 and VCAM-1, which are two of the most reported molecules involved in immune cell migration to the brain and spinal cord, are upregulated upon inflammation [44]. Thus, we examined the regulatory effect of NS on their expression in LPS-induced bEND.3 cells using real-time PCR analysis. MTT (3-[4,5-dimethylthiazol-2-yl]-2,5 diphenyl tetrazolium bromide) analysis demonstrated that NS (0.001–1600 μg/mL) did not decrease cell viability in bEnd.3 cells (Fig. 5A). The mRNA expressions of adhesive molecules, ICAM-1 and VCAM-1, were upregulated in LPS-stimulated bEND.3 cells (2.0 ± 0.1-fold and 9.1 ± 6.4-fold, respectively), and these upregulations were prevented by NS treatment (ICAM-1: 1.1 ± 0.1-fold and 1.2 ± 0.1-fold in the 100 and 200 mg/kg NS groups; VCAM-1: 1.9 ± 0.2-fold and 2.2 ± 0.2-fold in the 100 and 200 mg/kg groups) (Fig. 5B and C). Tight junctions between BBB endothelial cells build a powerful physical barrier whose breakdown underlies BBB dysfunction in several neurological disorders such as MS [1–3]. Thus, we explored the roles of NS on the expression of representative tight junction proteins (claudin-5 and occludin) in LPS-induced bEnd.3 cells. The mRNA expression of claudin-5 and occludin was significantly downregulated in LPS-stimulated bEND.3 cells. However, the downregulations were not significantly prevented by NS treatment (Fig. 5D and E). Our findings indicate that NS may reduce BBB permeability by inhibiting immune cell transmigration by decreasing the expression of cell adhesive molecules but not junctional molecules.

3.7. NS inhibits NF-κB and p38 MAPK pathways in LPS-stimulated bEND.3 cells

BBB permeability is essential in the pathology of MS and EAE [14,15]. Downregulating NF-κB and p38 MAPK pathways can ameliorate BBB permeability [45]. Thus, we evaluated the regulatory effect of NS on NF-κB and p38 MAPK kinase pathways in LPS-induced bEND.3 cells, a BBB cell line, to examine the effect of NS on BBB permeability (Fig. 6A–C). The protein expression levels of NF-κB p65 were remarkably upregulated in LPS-stimulated bEND.3 cells (93.8 ± 6.2 %), while their expression levels were significantly downregulated by NS in a dose-dependent manner (35.6 ± 10.1 % and 28.9 ± 4.7 % in EAE groups

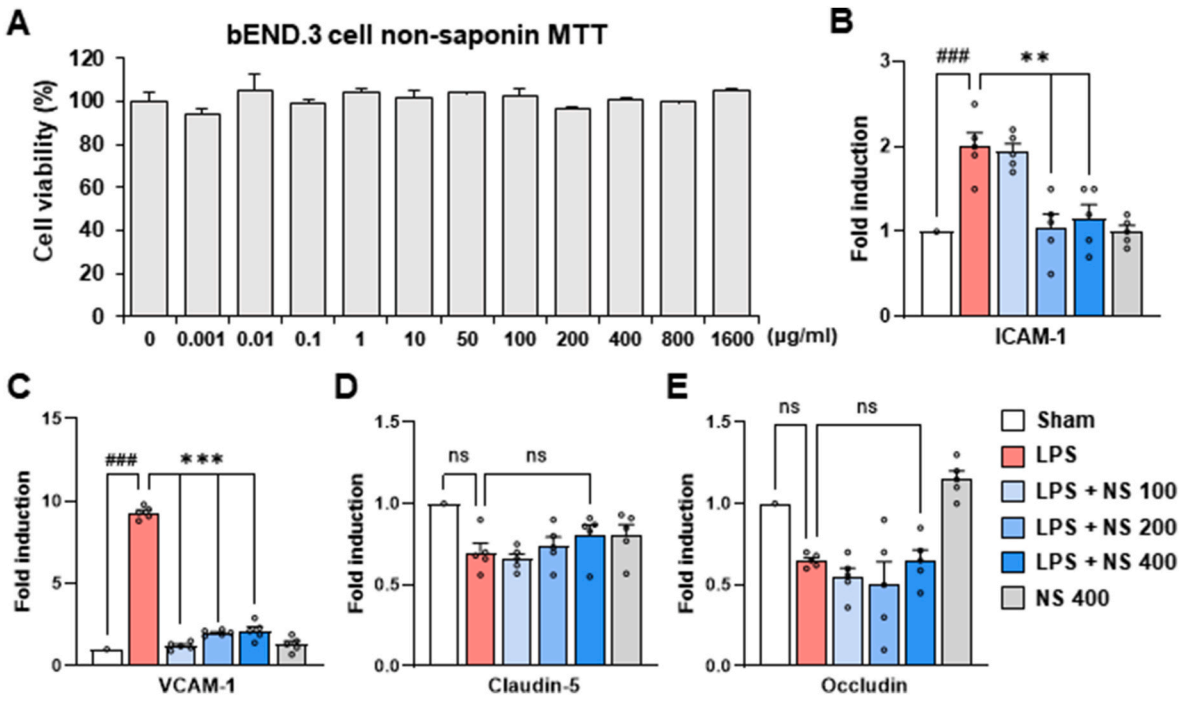

Fig. 5. NS downregulated cell adhesion molecules in LPS-induced bEND.3 cells.
(A) Cultured bEND.3 cells were treated with NS (0.001–1600 μg/mL) and harvested. Cell viability was investigated using the MTT assay. **(B–E)** bEND.3 cells were treated with NS (1, 10, and 100 μg/mL) 1 h before stimulation with LPS for 4 h. Harvested cells were assessed by real-time PCR analysis for mRNA expression levels of cell adhesion molecules ICAM-1 (B) and VCAM-1 (C) and tight junction molecules claudin-5 (D) and occludin (E). The experiment was repeated three times independently, and mRNA levels were normalized to GAPDHs levels (one-way ANOVA; $\#\#p < 0.01$, and $\#\#\#p < 0.001$ vs. sham group; $*p < 0.05$, $**p < 0.01$, and $***p < 0.001$ vs. EAE group). ANOVA, Analysis of variance; GAPDH, Glyceraldehyde 3-phosphate dehydrogenase; ICAM-1, Intercellular adhesion molecule-1; LPS, Lipopolysaccharide; ns, non-significant; NS, Non-saponin; VCAM-1, Vascular cell adhesion molecule-1.

treated wtih NS at 100 and 200 μg/mL, respectively) (Fig. 6A and B). The protein expression level of p38 MAPK was also unequivocally increased in LPS-stimulated bEND.3 cells (63.3 ± 6.2 %), but these decreases were prevented by treatment with NS (33.1 ± 4.7 % in EAE groups treated with NS at 200 μg/mL, respectively) (Fig. 6A and C).

4. Discussion

NSs prevented movement impairment (Fig. 2B–D), corresponding to the NS-induced mitigation of demyelination severity in mouse LSCs after EAE induction (Fig. 1E–I). NSs also decreased the infiltration of microglia, macrophages, and Th1 and Th17 cells (Figs. 2 and 3), reduced the expression of pro-inflammatory mediators (cytokines, chemokines, and enzymes) (Fig. 2H–M), and protected BBB integrity (Fig. 5) in LSCs from the EAE group. These valuable effects of NSs were related to the downregulation of the NF-κB and p38 MAPK pathways in LSCs from the EAE group and LPS-induced bEND.3 cells (Fig. 6). We believe that this was the first study to report that NSs might prevent movement disorders and LSC demyelination in EAE mice by upregulating anti-inflammatory activity and BBB permeability through the NF-κB and p38 MAPK pathways. These findings indicate that NSs could be considered a potential therapeutic agent for MS. Further research using MS patient-derived samples and various MS models is needed to validate these findings.

The severity of progressive movement disorders in MS patients and EAE models is intimately related to the severity of demyelinating (neurodegenerative) lesions in the spinal cord, which is associated with the level of migration and infiltration of microglia and macrophages around or within demyelinating sites [46]. Therefore, screening various drug candidates, such as herb-based agents and synthetic compounds, has been used to identify compounds that could prevent or cure neurodegenerative and inflammatory events in experimental (*in vitro and in vivo*) and clinical studies for MS [47]. Since no reliable medicines for MS are known, more effective and safer therapeutics are urgently needed [2,5,6]. Representative medicinal plants, such as *P. ginseng, Ginkgo biloba, Hypericum perforatum, Curcuma longa,* and their derivatives, might be developed as safe and reliable agents to treat MS by inhibiting neurodegeneration (demyelination) through their anti-inflammatory and neuroprotective effects [13,37,47]. KRGE, ginsenoside-Re, and ginseng-derived gintonin showed clear neuroprotective effects in EAE by exerting anti-inflammatory and antioxidant activity [33,37,39]. These previous reports indicate that ginseng-derived materials might exert favorable effects on MS and EAE. In the present study, NS administration noticeably alleviated the severity of movement disorders, demyelination, the infiltration of inflammatory cells, the migration of myeloid cells [microglia ($CD11b^+/CD45^{+(low)}$) and macrophages ($CD11b^+/CD45^{+(high)}$)], and the migration of T cell subsets (Th1 and Th17) in LSCs from the EAE group. These positive effects of NSs were related to the downregulation of the mRNA expression of representative pro-inflammatory cytokines (IL-1β), an enzyme (COX-2), and chemokines (MCP-1, MIP-1α, and RANTES) in LSCs from the EAE group.

The BBB plays a key role in inhibiting the influx of circulating mononuclear cells, such as macrophages and T cells, into the brain and spinal cord [48]. The BBB also plays a critical role in regulating the influx and efflux of biological substances to maintain the brain's homeostasis and neuronal role [48]. Because BBB permeability is one of the important characteristics of MS and EAE pathogenesis, factors that can regulate BBB permeability may be able to prevent or treat MS [14,15,49]. Here, the regulatory effect of NSs on BBB permeability was examined in LSCs from the EAE group and LPS-stimulated bEND.3 cells. NSs blocked astrocyte activation (a main component of the BBB) and the upregulation of PECAM-1 (a marker of BBB permeability) in LSCs from the EAE group, based on immunohistochemical and immunofluorescence staining and Western blot assays (Fig. 4). NSs also blocked the

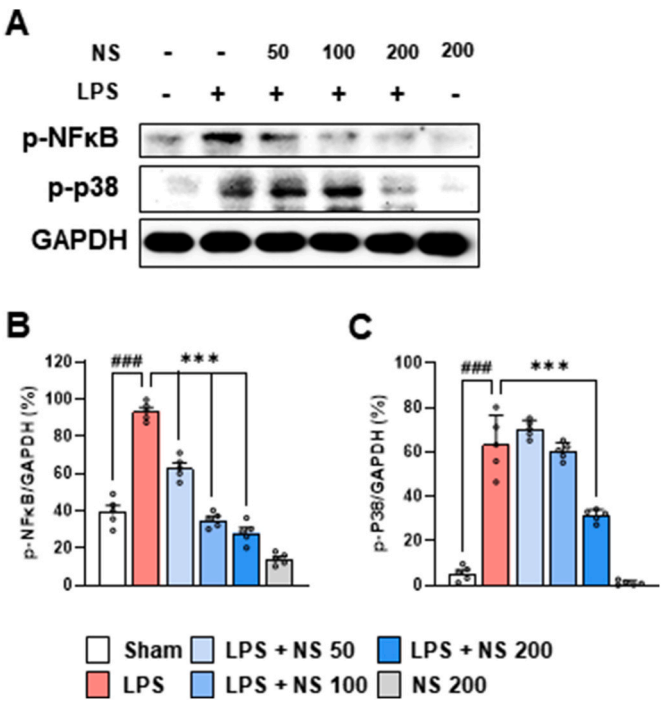

Fig. 6. NS inhibited NF-κB and p38 MAPK pathways in LPS-induced bEND.3 cells.
(A–C) Cultured bEND.3 cells were treated with NS (50, 100, and 200 μg/mL) 1 h before induction with LPS for 4 h. Cells were subjected to Western blot assay to examine protein expression grades of p-NF-kB p65 and p-p38 MAPK (A) followed by quantification (B and C). The experiment was repeated three times, and protein levels were normalized to GAPDH levels (one-way ANOVA; $\#\#p < 0.01$, and $\#\#\#p < 0.001$ vs. sham group; $^{*}p < 0.05$, $^{**}p < 0.01$, and $^{***}p < 0.001$ vs. EAE group). ANOVA, Analysis of variance; GAPDH, Glyceraldehyde 3-phosphate dehydrogenase; LPS, Lipopolysaccharide; NF-κB, Nuclear factor kappa-B; NS, Non-saponin; MAPK, Mitogen-activated protein kinase.

upregulation of ICAM-1 and VCAM-1 (representative markers of BBB permeability) without positive effects on downregulating claudin-5 and occludin (tight junctional molecules) in LPS-stimulated bEND.3 cells in real-time PCR assays (Fig. 5). These results were consistent with previous studies showing that the long-term oral administration of a gintonin-enriched fraction (a representative NS fraction) prevented increases in PECAM-1 in the cortex and hippocampus of Tg Alzheimer's disease mice [50]. Pathological BBB dysfunction was reported to amplify the development of neuroinflammation [51] and neuroimmune responses [52]. The NF-κB and p38 MAPK pathways play important roles in inflammatory and immune mechanisms underlying neurological diseases [53,54], as well as BBB malfunction mechanisms [45]. In the present study, NSs prevented the up-regulation of NF-κB and p38 MAPK pathways in LPS-stimulated bEND.3 cells, based on Western blot assays (Fig. 6). These findings could be indirectly explained by the following previous reports on NS: 1) Arginyl-fructosyl-glucose, a major Maillard reaction product of red ginseng blocked NF-κB-related apoptosis in cisplatin-induced acute kidney injury [27] and cisplatin-evoked intestinal toxicity [55]. 2) Gintonin, a ginseng-derived compound, inhibited NF-κB and p38 MAPK pathways in the brain and spinal cord of MOG_{35-55}-induced EAE and 3-NPA-induced striatal toxicity [56]. These findings suggest that NS might alleviate the transmigration and recruitment of peripheral immune cells, such as macrophages and T cells, by reducing the expression of cell adhesion molecules by inhibiting NF-κB and p38 MAPK pathways. Taken together, these results suggest NSs as a potential therapeutic agent, which may treat various neuroimmunological disorders, such as MS, and other neurodegenerative disorders, including AD, Parkinson's disease, and Huntington's disease, by regulating the NF-κB and p38 MAPK pathways.

5. Conclusion

NSs might mitigate movement impairment, one of the main symptoms of EAE. The effects were associated with the inhibition of neurodegeneration (demyelination), the infiltration of microglia and circulating immune cells (macrophages, CD4 T, Th1, and Th17 cells), and BBB permeability in LSCs by downregulating NF-κB and p38 MAPK signaling pathways. These results are the first to suggest NSs as a potential agent to prevent or treat inflammatory and autoimmune diseases, including MS. However, the efficacy and mechanism of action of NSs in various immunopathological conditions, including autoimmune diseases, as well as the chemical components and pharmacological roles of NSs, remain to be determined in experimental (*in vitro* and *in vivo*) and clinical studies.

Author contributions

JO: Methodology, Validation, Investigation, Visualization, and Writing–Original Draft. YH, Visualization, and Writing–Original Draft. SKM, YL, MSK, and SYN: Conceptualization, Supervision, Writing–Review & Editing. IHC: Conceptualization, Supervision, Resources, Writing–Review & Editing, and Funding acquisition. All data were generated in-house and no paper mill was used. All authors agree to be accountable for all aspects of this work and ensure its integrity and accuracy.

Declaration of competing interest

None of the authors of this manuscript have any conflicts of interest in this subject.

Acknowledgements

This research was supported by grant from the Korean Society of Ginseng, Republic of Korea (2019) and the National Research Foundation of Korea (NRF) grant funded by the Ministry of Science and ICT (NRF-2022R1A2C2009817).

References

[1] Filippi M, Bar-Or A, Piehl F, Preziosa P, Solari A, Vukusic S, et al. Multiple sclerosis. Nat Rev Dis Prim 2018;4:43.
[2] McGinley MP, Goldschmidt CH, Rae-Grant AD. Diagnosis and treatment of multiple sclerosis: a review. JAMA 2021;325:765–79.
[3] Reich DS, Lucchinetti CF, Calabresi PA. Multiple sclerosis. N Engl J Med 2018;378:169–80.
[4] Plastira I, Bernhart E, Goeritzer M, Reicher H, Kumble VB, Kogelnik N, et al. 1-Oleyl-lysophosphatidic acid (LPA) promotes polarization of BV-2 and primary murine microglia towards an M1-like phenotype. J Neuroinflammation 2016;13:205.
[5] Baecher-Allan C, Kaskow BJ, Weiner HL. Multiple sclerosis: mechanisms and immunotherapy. Neuron 2018;97:742–68.
[6] Huang WJ, Chen WW, Zhang X. Multiple sclerosis: pathology, diagnosis and treatments. Exp Ther Med 2017;13:3163–6.
[7] Adler AI, Knight H. Ocrelizumab for primary progressive multiple sclerosis. Lancet Neurol 2019;18:816–7.
[8] Mc Guire C, Prinz M, Beyaert R, van Loo G. Nuclear factor kappa B (NF-kappaB) in multiple sclerosis pathology. Trends Mol Med 2013;19:604–13.
[9] Leibowitz SM, Yan J. NF-kappaB pathways in the pathogenesis of multiple sclerosis and the therapeutic implications. Front Mol Neurosci 2016;9:84.
[10] Al-Griw MA, Salter MG, Wood IC. Blocking of NF-kB/p38 MAPK pathways mitigates oligodendrocyte pathology in a model of neonatal white matter injury. Acta Neurobiol Exp 2022;82:52–64.
[11] Cong H, Zhang M, Chang H, Du L, Zhang X, Yin L. Icariin ameliorates the progression of experimental autoimmune encephalomyelitis by down-regulating the major inflammatory signal pathways in a mouse relapse-remission model of multiple sclerosis. Eur J Pharmacol 2020;885:173523.
[12] Motawi TK, El-Maraghy SA, Kamel AS, Said SE, Kortam MA. Modulation of p38 MAPK and Nrf2/HO-1/NLRP3 inflammasome signaling and pyroptosis outline the anti-neuroinflammatory and remyelinating characters of Clemastine in EAE rat model. Biochem Pharmacol 2023;209:115435.
[13] Lee MJ, Chang BJ, Oh S, Nah SY, Cho IH. Korean Red Ginseng mitigates spinal demyelination in a model of acute multiple sclerosis by downregulating p38 mitogen-activated protein kinase and nuclear factor-kappaB signaling pathways. J Ginseng Res 2018;42:436–46.

[14] Ortiz GG, Pacheco-Moises FP, Macias-Islas MA, Flores-Alvarado LJ, Mireles-Ramirez MA, Gonzalez-Renovato ED, et al. Role of the blood-brain barrier in multiple sclerosis. Arch Med Res 2014;45:687–97.
[15] Balasa R, Barcutean L, Mosora O, Manu D. Reviewing the significance of blood-brain barrier disruption in multiple sclerosis pathology and treatment. Int J Mol Sci 2021;22.
[16] Li R. Natural product-based drug discovery. Med Res Rev 2016;36:3.
[17] Zhu Y, Ouyang Z, Du H, Wang M, Wang J, Sun H, et al. New opportunities and challenges of natural products research: when target identification meets single-cell multiomics. Acta Pharm Sin B 2022;12:4011–39.
[18] Choi JH, Lee YH, Kwon TW, Ko SG, Nah SY, Cho IH. Can Panax ginseng help control cytokine storm in COVID-19? J Ginseng Res 2022;46:337–47.
[19] Ratan ZA, Haidere MF, Hong YH, Park SH, Lee JO, Lee J, et al. Pharmacological potential of ginseng and its major component ginsenosides. J Ginseng Res 2021;45:199–210.
[20] Lee MJ, Choi JH, Oh J, Lee YH, In JG, Chang BJ, et al. Rg3-enriched Korean Red Ginseng extract inhibits blood-brain barrier disruption in an animal model of multiple sclerosis by modulating expression of NADPH oxidase 2 and 4. J Ginseng Res 2021;45:433–41.
[21] Hyun SH, Kim SW, Seo HW, Youn SH, Kyung JS, Lee YY, et al. Physiological and pharmacological features of the non-saponin components in Korean Red Ginseng. J Ginseng Res 2020;44:527–37.
[22] Kim S, Nam Y, Kim MJ, Kwon SH, Jeon J, Shin SJ, et al. Proteomic analysis for the effects of non-saponin fraction with rich polysaccharide from Korean Red Ginseng on Alzheimer's disease in a mouse model. J Ginseng Res 2023;47:302–10.
[23] Kim S, Shin SJ, Nam Y, Park YH, Kim BH, Park HH, et al. Korean red ginseng polysaccharide as a potential therapeutic agent targeting tau pathology in Alzheimer's disease. Int J Biol Macromol 2024;263:130516.
[24] Park K, Kim R, Cho K, Kong CH, Jeon M, Kang WC, et al. Panaxcerol D from Panax ginseng ameliorates the memory impairment induced by cholinergic blockade or Abeta(25-35) peptide in mice. J Ginseng Res 2024;48:59–67.
[25] Lee A, Kwon OW, Jung KR, Song GJ, Yang HJ. The effects of Korean Red Ginseng-derived components on oligodendrocyte lineage cells: distinct facilitatory roles of the non-saponin and saponin fractions, and Rb1, in proliferation, differentiation and myelination. J Ginseng Res 2022;46:104–14.
[26] Zhang JJ, Chen KC, Yin JY, Zheng YN, Chen RX, Liu W, et al. AFG, an important maillard reaction product in red ginseng, alleviates D-galactose-induced brain aging in mice via correcting mitochondrial dysfunction induced by ROS accumulation. Eur J Pharmacol 2023;952:175824.
[27] Li RY, Zhang WZ, Yan XT, Hou JG, Wang Z, Ding CB, et al. Arginyl-fructosyl-glucose, a major maillard reaction product of red ginseng, attenuates cisplatin-induced acute kidney injury by regulating nuclear factor kappaB and phosphatidylinositol 3-kinase/protein kinase B signaling pathways. J Agric Food Chem 2019;67:5754–63.
[28] Liu X, Liu W, Ding C, Zhao Y, Chen X, Khatoon S, et al. Antidiabetic effects of arginyl-fructosyl-glucose, a nonsaponin fraction from ginseng processing in streptozotocin-induced type 2 diabetic mice through regulating the PI3K/AKT/GSK-3beta and Bcl-2/Bax signaling pathways. Evid Based Complement Alternat Med 2020;2020:3707904.
[29] Cho JH, Song MC, Lee Y, Noh ST, Kim DO, Rha CS. Newly identified maltol derivatives in Korean Red Ginseng and their biological influence as antioxidant and anti-inflammatory agents. J Ginseng Res 2023;47:593–603.
[30] Park SJ, Lee D, Kim D, Lee M, In G, Han ST, et al. The non-saponin fraction of Korean Red Ginseng (KGC05P0) decreases glucose uptake and transport in vitro and modulates glucose production via down-regulation of the PI3K/AKT pathway in vivo. J Ginseng Res 2020;44:362–72.
[31] In G, Ahn NG, Bae BS, Lee MW, Park HW, Jang KH, et al. In situ analysis of chemical components induced by steaming between fresh ginseng, steamed ginseng, and red ginseng. J Ginseng Res. 2017;41:361–9.
[32] Landis SC, Amara SG, Asadullah K, Austin CP, Blumenstein R, Bradley EW, et al. A call for transparent reporting to optimize the predictive value of preclinical research. Nature 2012;490:187–91.
[33] Oh J, Kwon TW, Choi JH, Kim Y, Moon SK, Nah SY, et al. Ginsenoside-Re inhibits experimental autoimmune encephalomyelitis as a mouse model of multiple sclerosis by downregulating TLR4/MyD88/NF-kappaB signaling pathways. Phytomedicine 2024;122:155065.
[34] Choi JH, Oh J, Lee MJ, Bae H, Ko SG, Nah SY, et al. Inhibition of lysophosphatidic acid receptor 1-3 deteriorates experimental autoimmune encephalomyelitis by inducing oxidative stress. J Neuroinflammation 2021;18:240.
[35] Lee MJ, Jang M, Choi J, Lee G, Min HJ, Chung WS, et al. Bee venom acupuncture alleviates experimental autoimmune encephalomyelitis by upregulating regulatory T cells and suppressing Th1 and Th17 responses. Mol Neurobiol 2016;53:1419–45.
[36] Lee MJ, Bing SJ, Choi J, Jang M, Lee G, Lee H, et al. IKKbeta-mediated inflammatory myeloid cell activation exacerbates experimental autoimmune encephalomyelitis by potentiating Th1/Th17 cell activation and compromising blood brain barrier. Mol Neurodegener 2016;11:54.
[37] Lee MJ, Jang M, Choi J, Chang BS, Kim do Y, Kim SH, et al. Korean red ginseng and ginsenoside-Rb1/-rg1 alleviate experimental autoimmune encephalomyelitis by suppressing Th1 and Th17 cells and upregulating regulatory T cells. Mol Neurobiol 2016;53:1977–2002.
[38] Choi JH, Lee MJ, Jang M, Kim EJ, Shim I, Kim HJ, et al. An oriental medicine, hyungbangpaedok-san attenuates motor paralysis in an experimental model of multiple sclerosis by regulating the T cell response. PLoS One 2015;10:e0138592.
[39] Choi JH, Oh J, Lee MJ, Ko SG, Nah SY, Cho IH. Gintonin mitigates experimental autoimmune encephalomyelitis by stabilization of Nrf2 signaling via stimulation of lysophosphatidic acid receptors. Brain Behav Immun 2021;93:384–98.
[40] Sasaki Y, Ohsawa K, Kanazawa H, Kohsaka S, Imai Y. Iba1 is an actin-cross-linking protein in macrophages/microglia. Biochem Biophys Res Commun 2001;286:292–7.
[41] Sonar SA, Lal G. Differentiation and transmigration of CD4 T cells in neuroinflammation and autoimmunity. Front Immunol 2017;8:1695.
[42] Hoglund RA, Maghazachi AA. Multiple sclerosis and the role of immune cells. World J Exp Med 2014;4:27–37.
[43] Milovanovic J, Arsenijevic A, Stojanovic B, Kanjevac T, Arsenijevic D, Radosavljevic G, et al. Interleukin-17 in chronic inflammatory neurological diseases. Front Immunol 2020;11:947.
[44] Lecuyer MA, Kebir H, Prat A. Glial influences on BBB functions and molecular players in immune cell trafficking. Biochim Biophys Acta 2016;1862:472–82.
[45] Dong L, Qiao H, Zhang X, Zhang X, Wang C, Wang L, et al. Parthenolide is neuroprotective in rat experimental stroke model: downregulating NF-kappaB, phospho-p38MAPK, and caspase-1 and ameliorating BBB permeability. Mediat Inflamm 2013;2013:370804.
[46] Wang J, Wang J, Wang J, Yang B, Weng Q, He Q. Targeting microglia and macrophages: a potential treatment strategy for multiple sclerosis. Front Pharmacol 2019;10:286.
[47] Mojaverrostami S, Bojnordi MN, Ghasemi-Kasman M, Ebrahimzadeh MA, Hamidabadi HG. A review of herbal therapy in multiple sclerosis. Adv Pharmaceut Bull 2018;8:575–90.
[48] Kadry H, Noorani B, Cucullo L. A blood-brain barrier overview on structure, function, impairment, and biomarkers of integrity. Fluids Barriers CNS 2020;17:69.
[49] Malkiewicz MA, Szarmach A, Sabisz A, Cubala WJ, Szurowska E, Winklewski PJ. Blood-brain barrier permeability and physical exercise. J Neuroinflammation 2019;16:15.
[50] Jang M, Choi SH, Choi JH, Oh J, Lee RM, Lee NE, et al. Ginseng gintonin attenuates the disruptions of brain microvascular permeability and microvascular endothelium junctional proteins in an APPswe/PSEN-1 double-transgenic mouse model of Alphalzheimer's disease. Exp Ther Med 2021;21:310.
[51] Takata F, Nakagawa S, Matsumoto J, Dohgu S. Blood-brain barrier dysfunction amplifies the development of neuroinflammation: understanding of cellular events in brain microvascular endothelial cells for prevention and treatment of BBB dysfunction. Front Cell Neurosci 2021;15:661838.
[52] Banks WA. The blood-brain barrier in neuroimmunology: tales of separation and assimilation. Brain Behav Immun 2015;44:1–8.
[53] Cao LH, Zhao YY, Bai M, Geliebter D, Geliebter J, Tiwari R, et al. Mechanistic studies of gypenosides in microglial state transition and its implications in depression-like behaviors: role of TLR4/MyD88/NF-kappaB signaling. Front Pharmacol 2022;13:838261.
[54] Zhao J, Bi W, Zhang J, Xiao S, Zhou R, Tsang CK, et al. USP8 protects against lipopolysaccharide-induced cognitive and motor deficits by modulating microglia phenotypes through TLR4/MyD88/NF-kappaB signaling pathway in mice. Brain Behav Immun 2020;88:582–96.
[55] Liu W, Zhang H, Hou YY, Hu RY, Zhang JJ, Chen X, et al. Arginyl-fructosyl-glucose, a major Maillard reaction product of red ginseng mitigates cisplatin-evoked intestinal toxicity in vivo and in vitro. Food Funct 2022;13:11283–97.
[56] Jang M, Choi JH, Chang Y, Lee SJ, Nah SY, Cho IH. Gintonin, a ginseng-derived ingredient, as a novel therapeutic strategy for Huntington's disease: activation of the Nrf2 pathway through lysophosphatidic acid receptors. Brain Behav Immun 2019;80:146–62.